Chemical Kinetics of Reactions in the Unfrozen Solution of Ice

Norimichi Takenaka* and Hiroshi Bandow

Laboratory of Environmental Chemistry, Graduate School of Engineering, Osaka Prefecture University, Gakuen-cho 1-1, Sakai-shi, Osaka 599-8531, Japan

Received: May 18, 2007; In Final Form: June 28, 2007

Some reactions are accelerated in ice compared to aqueous solution at higher temperatures. Accelerated reactions in ice take place mainly due to the freeze-concentration effect of solutes in an unfrozen solution at temperatures higher than the eutectic point of the solution. Pincock was the first to report an acceleration model for reactions in ice,[1] which successfully simulated experimental results. We propose here a modified version of the model for reactions in ice. The new model includes the total molar change involved in reactions in ice. Furthermore, we explain why many reactions are not accelerated in ice. The acceleration of reactions can be observed in the cases of (i) second- or higher-order reactions, (ii) low concentrations, and (iii) reactions with a small activation energy. Reactions with a buffer solution or additives in order to adjust ion strength, zero- or first-order reactions, or reactions containing high reactant concentrations are not accelerated by freezing. We conclude that the acceleration of reactions in the unfrozen solution of ice is not an abnormal phenomenon.

Introduction

Rates of chemical reactions in aqueous solution are generally suppressed with decreasing temperature. However, some reactions are accelerated in ice despite being at lower temperatures than in solution.[1−24] The acceleration of reactions in ice has been studied actively since the 1960s in the field of food chemistry and biochemistry, where acceleration mechanisms were reported. Pincock reviewed the reactions in frozen systems[1] and concluded that freeze-concentration in an unfrozen solution of ice was the only cause of acceleration in such systems. A systematic review of the acceleration mechanism is summarized by Fennema as follows.[11] (1) Freeze-concentration: the large majority of solutes are rejected from ice crystal lattices and are concentrated in the unfrozen solution of ice, and the reactions are accelerated. (2) Freezing potential: only small amounts of solutes are incorporated in ice crystals, and the difference in cation and anion incorporation between ice crystals and the unfrozen solution generates an electric potential. Freezing potentials, with respect to ice, have been reported as +214 to −90 V.[25,26] Electrochemical reactions take place by the potential generated. (3) Hydrolysis by changing pH value as a result of neutralization of the freezing potential: H^+ or OH^- transfers from the ice crystals to the unfrozen solution or the unfrozen solution to the ice crystals in order to neutralize the freezing potential, and hydrolysis reactions take place. 4) The others: the catalytic reaction of ice, preferred orientation of reactants in ice, and difference in dielectric constants between water and ice are reported. Fennema concluded that among these mechanisms, the freeze-concentration into the unfrozen solution in ice is a main cause of acceleration.[11] In our previous work, various possibilities causing the acceleration of the reaction of nitrous acid with dissolved oxygen were investigated.[16] Finally, it was concluded that the acceleration occurs due to the freeze-concentration of solutes, contained in the unfrozen solution of ice, in regions called micropockets. However, with the above-mentioned mechanism, it is difficult to understand why acceleration of reactions in micropockets for most reactions is not observed.

Pincock reported the first model of the acceleration mechanism in the unfrozen solution of ice by incorporating the freeze-concentration effect.[1] Using the model, reaction rates were quantified and shown to be in good agreement with the experimental results. The model reported by Pincock, however, does not include the effect of molar change during reactions. In the present paper, Pincock's model is modified by considering the molar change by the reaction. Furthermore, some aspects derived from the model are shown in order to explain that the acceleration in ice is not an unusual phenomenon but takes place only under special conditions and reaction mechanisms. The present paper shows why the acceleration of reactions in ice for most reactions is not observed. It is expected that reactions accelerated in ice can be quantified using the proposed mechanism.

Model of Kinetics in the Micropocket

Reaction 1 of A and B is considered.

$$aA + bB \rightarrow \text{products} \quad (1)$$

Here, a and b are the molar coefficients for A and B, respectively. The reaction rate is expressed as

$$\text{rate} = k[A]^a[B]^b \quad (2)$$

Here k is a rate coefficient and is expressed as

$$k = A \exp(-E_a/RT) \quad (3)$$

Here, A is a pre-exponential factor, E_a is the activation energy of reaction 1, R is the gas constant, and T is the absolute temperature.

* To whom correspondence should be addressed. Phone: (+81)72-254-9322. Fax: (+81)72-254-9910. E-mail: takenaka@chem.osakafu-u.ac.jp.

10.1021/jp0738356 CCC: $37.00
Published on Web 08/17/2007

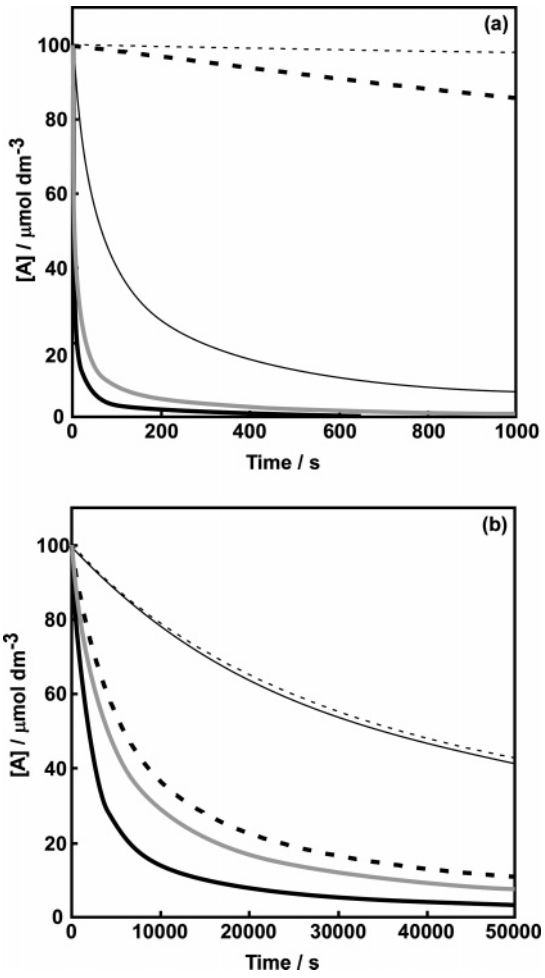

Figure 1. Time profile of reactant A in the second-order reaction in ice with 50 kJ mol^{-1} of the activation energy at various temperatures in the case without a change in the number of moles by the reaction 2A → 2P. The results at 25 and 0 °C in the solution are also shown in the figure for comparison. Temperature in the micropocket: thick solid black line, −15 °C; thick solid gray line, −2 °C; fine solid black line, −0.2 °C. Temperature in the solution: thick broken line, 25 °C; fine broken line, 0 °C in the solution. The activation energy and pre-exponential factor of the reaction are 50 kJ mol^{-1} and 1×10^9 mol^{-1} dm^3 s^{-1}, respectively. The initial concentration of reactant A is 1×10^{-4} mol dm^{-3}. The total concentrations of the species existing in the solution are (a) 2×10^{-4} mol dm^{-3} and (b) 1×10^{-1} mol dm^{-3}.

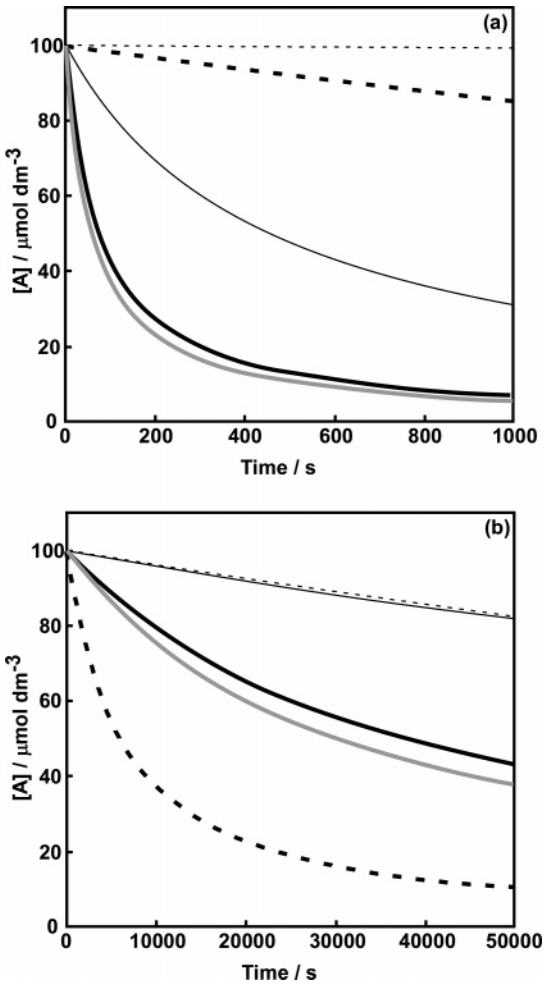

Figure 2. Time profile of reactant A in the second-order reaction in ice with 100 kJ mol^{-1} of the activation energy at various temperatures in the case without a change in the number of moles by the reaction 2A → 2P. The results at 25 and 0 °C in the solution are also shown in the figure for comparison. Temperature in the micropocket: thick solid black line, −15 °C; thick solid gray line, −2 °C; fine solid black line, −0.2 °C. Temperature in the solution: thick broken line, 25 °C; fine broken line, 0 °C in the solution. The activation energy and pre-exponential factor of the reaction are 100 kJ mol^{-1} and 5.8×10^{17} mol^{-1} dm^3 s^{-1}, respectively. The initial concentration of reactant A is 1×10^{-4} mol dm^{-3}. The total concentrations of the species existing in the solution are (a) 2×10^{-4} mol dm^{-3} and (b) 1×10^{-1} mol dm^{-3}. The pre-exponential factor is adjusted to be the same reaction rate as that in the Figure 1.

If all solutes are assumed to be rejected from ice crystals to the unfrozen solution of ice, the concentrations of solutes A and B in the micropockets in the frozen ice, $[A]_f$ and $[B]_f$, respectively, can be expressed as follows:

$$[A]_f = [A]\frac{C_{fp}}{C_T}$$

$$[B]_f = [B]\frac{C_{fp}}{C_T} \quad (4)$$

Here, C_T denotes the sum of the concentration of all solutes in the solution, and C_{fp} is the total concentration in the micropockets and is determined from the equilibrium diagram of the solution and solid ice. Near the freezing point of water it is determined by the freezing point depression: $C_{fp} = \Delta T(d/1.86)$, where d denotes the density of the solution in the micropockets in kg dm^{-3}. For simplicity, it is assumed that C_{fp} is equal to the activity at any concentration. The reaction rate of 1 in the micropocket, R_f, is expressed as

$$R_f = k[A]_f^a[B]_f^b = k\left(\frac{C_{fp}}{C_T}[A]\right)^a\left(\frac{C_{fp}}{C_T}[B]\right)^b \quad (5)$$

Here, R_f is a reaction rate when a reaction proceeds in the micropockets. The total volume of the micropockets V_f can be expressed as

$$V_f = \frac{C_T}{C_{fp}}V_s \quad (6)$$

Here, V_s denotes a volume of the original solution. The acceleration of reactions in micropockets was usually observed after the sample was melted. After the sample is melted, solute concentrations are diluted by a factor of V_f/V_s. If x is taken as the concentration of A that is measured after the sample is

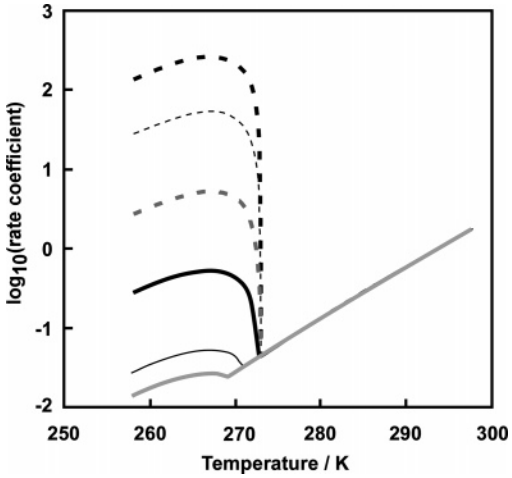

Figure 3. Temperature dependence of the rate coefficients at various total concentrations. Total concentration: thick black broken line, 2×10^{-4} mol dm^{-3}; fine broken line, 1×10^{-3} mol dm^{-3}; thick gray broken line, 1×10^{-2} mol dm^{-3}; thick black solid line, 1×10^{-1} mol dm^{-3}; fine black solid line, 1 mol dm^{-3}; thick gray solid line, 2 mol dm^{-3}. The initial concentration of reactant A is 100 μmol dm^{-3}. The activation energy and pre-exponential factor of the reaction are 100 kJ mol^{-1} and 5.8×10^{17} mol^{-1} dm^3 s^{-1}, respectively.

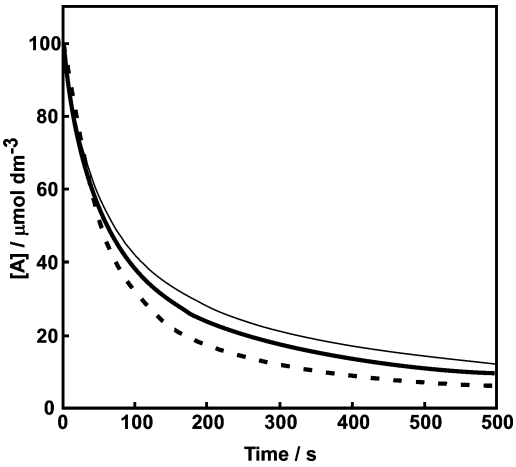

Figure 4. Time profile of the concentration on reactant A with and without a change in the total number of moles by the reaction in the unfrozen solution of ice. The initial total concentration and concentration of reactant A are 2×10^{-4} and 1×10^{-4} mol dm^{-3}, respectively. The activation energy and pre-exponential factor of the reaction are 100 kJ mol^{-1} and 5.8×10^{17} mol^{-1} dm^3 s^{-1}, respectively. The temperature is -2 °C. Thick solid line: no change in the total number of moles by the reaction 2A → 2P. Fine solid line: increase in the total moles by the reaction 2A → 3P. Thick broken line: decrease in the total number of moles by the reaction 2A → P.

melted, the reaction rate measured after thawing, R_m, is expressed as

$$R_m = \frac{dx}{dt} = k\left(\frac{C_{fp}}{C_T}[A]\right)^a\left(\frac{C_{fp}}{C_T}[B]\right)^b\frac{V_f}{V_s} = k\left(\frac{C_{fp}}{C_T}([A]_0 - x)\right)^a\left(\frac{C_{fp}}{C_T}\left([B]_0 - \frac{b}{a}x\right)\right)^b\frac{C_T}{C_{fp}} \quad (7)$$

Here, $[A]_0$ and $[B]_0$ are the initial concentrations of A and B, respectively. Equation 7 has the same form as that reported by Pincock.[1] The total concentration in the micropockets is changed when the reaction proceeds according to the molar change by the reaction. When the initial total concentration is expressed as C_{T0} and the molar change due to the reaction is expressed as ΔC, the reaction rate measured after thawing can be written as

$$\frac{dx}{dt} = k\left(\frac{C_{fp}}{C_{T0} + \Delta C}([A]_0 - x)\right)^a\left(\frac{C_{fp}}{C_{T0} + \Delta C}\left([B]_0 - \frac{b}{a}x\right)\right)^b\frac{C_{T0} + \Delta C}{C_{fp}} \quad (8)$$

The reaction rate of 1 in the micropocket is governed by eq 8.

Note, at temperatures lower than the eutectic temperature of the system, the above mechanism should not be applied. Diffusion of solutes in ice has been reported recently below the eutectic point.[27−31] Furthermore, it has been reported that the quisi-brine layer still exists below the eutectic point.[27−31] However, the mechanism of reactions below the eutectic temperature has not been well understood so far. We restrict the application of eq 8 between the freezing temperature of the initial solution and the eutectic temperatures of the unfrozen solutions.

Results and Discussion

On the basis of eq 8, various reaction mechanisms in solution are expressed as in the case of reactions in ice, and we show what kinds of reactions are accelerated in ice.

(1) First-Order Reaction without Change in the Total Concentration by the Reaction, A → P. A change in the total concentration of species does not occur. Therefore, eq 8 can be expressed as eq 9.

$$\frac{dx}{dt} = k\left\{\frac{C_{fp}}{C_{T0}}([A]_0 - x)\right\}\frac{C_{T0}}{C_{fp}} = k([A]_0 - x) \quad (9)$$

Here, x is defined as the concentration of A reacted. The integral form of eq 9 is

$$\ln\frac{[A]_0}{[A]_0 - x} = kt \quad (10)$$

Equation 10 has the same form as that in the solution and, therefore, the reaction is not accelerated in the unfrozen solution in ice when the activation energy is positive. In other words, in the case of the first-order reaction, the rate equations of the reactions, accompanying a change in the total concentration in the unfrozen solution of ice, are also the same as those in solution. The reaction rate in the unfrozen solution also obeys the temperature dependence of the solution. The lack of acceleration of the first-order reaction by freezing was reported by Kiovsky and Pincock.[32]

(2) Second-Order Reaction without Change in the Total Concentration by the Reaction, 2A → 2P. A change in the total concentration of species does not occur. Equation 8 can be expressed as

$$\frac{dx}{dt} = k\left\{\frac{C_{fp}}{C_{T0}}([A]_0 - x)\right\}^2\frac{C_{T0}}{C_{fp}} = k([A]_0 - x)^2\frac{C_{fp}}{C_{T0}} \quad (11)$$

The integrated form of the eq 11 is

$$\frac{x}{[A]_0([A]_0 - x)} = \frac{kC_{fp}}{C_{T0}}t \quad (12)$$

The calculated results at -0.2, -2, and -15 °C with $E_a = 50$ kJ mol^{-1} are shown in Figure 1, with those in the solution at

TABLE 1: Rate Equations of Several Reactions

reaction[a]	rate equation[b] $dx/dt =$	integrated form[b] $kt =$
A → P	$k([A]_0 - x)$	$\ln \frac{[A]_0}{[A]_0 - x}$
A → 2P	$k([A]_0 - x)$	$\ln \frac{[A]_0}{[A]_0 - x}$
2A → P	$k([A]_0 - x)^2 \frac{C_{fp}}{(C_{T0} - x)}$	$\frac{1}{C_{fp}}\left(\frac{(C_{T0} - [A]_0)x}{([A]_0 - x)[A]_0} - \ln \frac{[A]_0 - x}{[A]_0}\right)$
2A → 2P	$k([A]_0 - x)^2 \frac{C_{fp}}{C_{T0}}$	$\frac{x}{([A]_0 - x)[A]_0} \frac{C_{T0}}{C_{fp}}$
2A → 3P	$k([A]_0 - x)^2 \frac{C_{fp}}{C_{T0} + x}$	$\frac{1}{C_{fp}}\left(\frac{(C_{T0} + [A]_0)x}{([A]_0 - x)[A]_0} + \ln \frac{[A]_0 - x}{[A]_0}\right)$
2A → *n*P	$k([A]_0 - x)^2 \frac{C_{fp}}{C_{T0} + (n-2)x}$	$\frac{1}{C_{fp}}\left(\frac{(C_{T0} + (n-2)[A]_0)x}{([A]_0 - x)[A]_0} + (n-2)\ln \frac{[A]_0 - x}{[A]_0}\right)$
A + B → P	$k([A]_0 - x)([B]_0 - x) \frac{C_{fp}}{C_{T0} - x}$	$\frac{1}{C_{fp}} \frac{1}{([A]_0 - [B]_0)}\left[-(C_{T0} - [A]_0)\ln \frac{[A]_0}{([A]_0 - x)} + (C_{T0} - [B]_0)\ln \frac{[B]_0}{([B]_0 - x)}\right]$
A + B → 2P	$k([A]_0 - x)([B]_0 - x) \frac{C_{fp}}{C_{T0}}$	$\frac{C_{T0}}{C_{fp}}\left[\frac{1}{([A]_0 - [B]_0)}\ln \frac{([A_0] - x)[B]_0}{([B]_0 - x)[A]_0}\right]$
A + B → 3P	$k([A]_0 - x)([B]_0 - x) \frac{C_{fp}}{C_{T0} + x}$	$\frac{1}{C_{fp}} \frac{1}{([A]_0 - [B]_0)}\left[-(C_{T0} + [A]_0)\ln \frac{[A]_0}{([A]_0 - x)} + (C_{T0} + [B]_0)\ln \frac{[B]_0}{([B]_0 - x)}\right]$

[a] A and B are reactants. P indicates a product, and species of products are not distinguished. If two kinds of products are formed, it is represented as 2P and not P1 + P2. [b] For each symbol, see text.

25 and 0 °C. Figure 1a shows the results at a total concentration of 2×10^{-4} mol dm^{-3} and an initial concentration of reactant A of 1×10^{-4} mol dm^{-3}. The reaction rates in the micropocket at lower temperatures are much faster than those in the solutions at higher temperatures. In this case, the acceleration of the reaction rate in the unfrozen solution of ice can be observed. Figure 1b shows those with the total concentration of 0.1 mol dm^{-3} and an initial concentration of A equal to 1×10^{-4} mol dm^{-3}. The total concentration in Figure 1b is much higher than that in Figure 1a. The reaction rates at 25 and 0 °C in Figure 1b are the same as those at 25 and 0 °C in Figure 1a, respectively. In Figure 1b, the reaction rate at −2 °C is almost the same as that at 25 °C. It is difficult to observe the acceleration of the reaction in the micropockets when considering the time in the liquid state of the sample (e.g., the time prior to freezing and the time after thawing until analysis). Figure 2 shows the calculated results under the same conditions as Figure 1 except that $E_a = 100$ kJ mol^{-1}. Panels a and b of Figure 2 show results at total concentrations of 2×10^{-4} mol dm^{-3} and 1×10^{-1} mol dm^{-3}, respectively. The pre-exponential factor is adjusted to produce the same reaction rate at 25 °C as that in Figure 1. Thus, the reaction rates in the solution at 25 °C are the same in the four figures (i.e., Figures 1a,b and 2a,b). In Figure 2a, the reaction rates in ice are faster than those in solution, but the effects are smaller than those in reaction with lower E_a. Conversely, in Figure 2b, the reaction rate at 25 °C in the solution is faster than those in the unfrozen solution in the ice. In this case also, the acceleration of the reaction in the ice or by freezing cannot be observed.

Figure 3 shows the change in the reaction rate coefficients with temperature at various total concentrations. The reaction rate coefficients of reactions in ice increase with decreasing temperature, reach to the maximum at a certain temperature (−6 °C in the case of Figure 3), and decrease with decreasing temperature. When the freezing point of the sample solution is lower than the temperature at which the maximum rate coefficient is obtained, the rate coefficient in ice decreases with decreasing temperature without any rate coefficient peak. On the other hand, when the eutectic temperature of the sample solution is higher than the temperature at which the maximum rate coefficient is obtained, the rate coefficient in ice increases with decreasing temperature without any rate coefficient peak.

In Figure 3, the concentration of reactant A is 1×10^{-4} mol dm^{-3}. When the total concentrations are low, the reaction rates in the ice are much faster than those in the solution, while at high total concentrations, the reaction rates in the ice are not very fast, compared to those in the solution. In the case of high total concentration, the ratio of $[A]_f$ to C_{fp} is low, and the reaction is slow due to the low freeze-concentration effect for reactant A. In most studies of reactions in solution, the addition of buffer solution and/or a high concentration of additional salts to adjust ion strength are used, and therefore, the acceleration in ice cannot be observed due to the high concentrations produced. This is probably the main reason why the acceleration

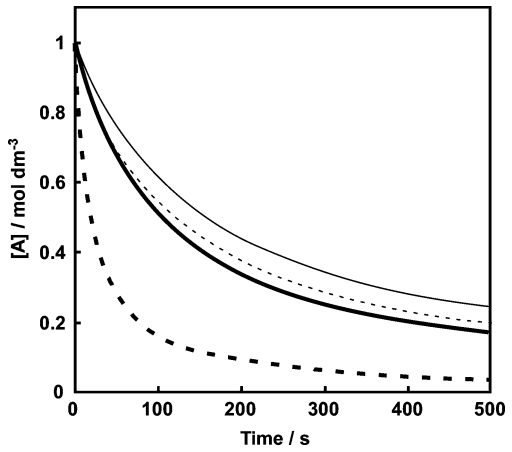

Figure 5. Time profile of the concentration on reactant A in the case of the high reactant concentration (2A → 2P). The results at 25 and 0 °C in the solution are also shown in the figure for comparison. Temperature in the micropocket: thick solid line, −11 °C; fine solid line, −4 °C. Temperature in the solution: thick broken line, 25 °C; fine broken line, 0 °C. The activation energy and pre-exponential factor of the reaction are 50 kJ mol^{-1} and 3×10^7 mol^{-1} dm^3 s^{-1}, respectively. The initial concentration of reactant A is 1 mol dm^{-3}. The total concentration of the species existing in the solution is 2 mol dm^{-3}. The freezing point of the solution is assumed to be −3.8 °C.

of reactions in the ice are not well known in general. In Figure 2a,b, the reaction rate at −15 °C is slower than that at −2 °C. This can be confirmed in Figure 3; that is, the maximum reaction rate can be obtained at a certain temperature. This result was also shown by Pincock.[1] The temperature at which the maximum reaction rate is observed depends on the reaction mechanism, magnitude of the freeze concentration effect, and the value of the activation energy. In the case of Figure 3, the first two factors are the same in all cases, and only the freeze-concentration effect controls the reaction rate. In this case, the freeze-concentration effect is proportional to the ratio of concentration of the reactant to total concentration, and the reaction rate coefficients peaks are observed at the same temperature. When the reaction has the lower activation energy, the temperature that exhibits the maximum reaction rate is lower or showed no maximum until the eutectic point of the solution. Thus, the eutectic point, the temperature exhibiting the maximum reaction rate (i.e., governed by E_a), the total concentration, and the initial reactant concentration are important factors controlling the reaction rate in ice.

(3) Second-Order Reaction with a Decrease in the Total Concentration by the Reaction, 2A → P. The change in the total concentration of species is $-x$.

$$\frac{dx}{dt} = k\left\{\frac{C_{fp}}{C_{T0} - x}([A]_0 - x)\right\}^2 \frac{C_{T0} - x}{C_{fp}} = k\frac{([A]_0 - x)^2}{(C_{T0} - x)}C_{fp} \quad (13)$$

The integrated form of eq 13 is

$$\frac{(C_{T0} - [A]_0)x}{([A]_0 - x)[A]_0} - \ln\frac{[A]_0 - x}{[A]_0} = kC_{fp}t \quad (14)$$

(4) Second-Order Reaction with an Increase in the Total Concentration by the Reaction, 2A → 3P. The change in the total concentration of species is $+x$.

$$\frac{dx}{dt} = k\left\{\frac{C_{fp}}{C_{T0} + x}([A]_0 - x)\right\}^2 \frac{C_{T0} + x}{C_{fp}} = k\frac{([A]_0 - x)^2}{(C_{T0} + x)}C_{fp} \quad (15)$$

The integrated form of the eq 15 is

$$\frac{(C_{T0} + [A]_0)x}{([A]_0 - x)[A]_0} + \ln\frac{[A]_0 - x}{[A]_0} = kC_{fp}t \quad (16)$$

The time profiles of the observed concentration of reactant A with and without change in the total concentration by the reactions in ice are shown in Figure 4. The effect of the change in the total concentration by the reaction is not very large and is smaller at higher total concentration. When the total concentration decreases by the reaction, the reaction is the fastest among the three. This is due to the increase in the relative concentration of reactant A as the reaction proceeds. The total concentration in the unfrozen solution in the ice is dominated by the temperature, specifically, the solid/liquid equilibrium.

(5) Higher-Order Reactions. From the above results, it is clear that the acceleration depends on $[C_{fp}/(C_{T0} + px)]^{(n-1)}$. Here, px is a molar change by the reaction, and n is the reaction order. Therefore, the higher-order reaction is expected to be extremely accelerated by the freezing. The rate equations of each reaction order are summarized in Table 1.

(6) Pseudo-First-Order Reaction. The pseudo first-order reactions are usually treated as the first-order reactions in solution since one of the reactants is constant. In the calculation, the concentration of this reactant is combined with a rate coefficient, for example $k' = k[A]$. In the case of pseudo-first-order reactions without molar change due to the reactions, it is possible to perform the same treatment, that is, combine the term for the constant concentration of the reactant with a rate coefficient. However, for reactions with molar change by reactions, they cannot be treated as pseudo first-order reactions but must be treated as the second- or the higher-order reactions, because the apparent reaction rate coefficient, k', is also changed by reactions.

(7) High Concentration of the Reactant. Figure 5 shows the time profile of the concentration of reactant A in the circumstance of a high initial concentration of A, that is, 1.0 mol dm^{-3} of reactant A and 2.0 mol dm^{-3} of the total concentration in the case of no molar change of the second-order reaction (2A → 2P). In this case also, the reaction at 25 °C is faster than the reactions in the unfrozen solution in ice. Similar results can also be observed in Figure 3, although the pre-exponential factor and E_a are different. Under the condition of Figure 5, the maximum rates in ice are obtained at −11 °C. In the case of the second-order reaction without molar change by the reaction, the rate coefficient measured after thawing, k', is represented as

$$k' = k\frac{C_{fp}}{C_T} = A\exp(-E_a/RT)\frac{C_{fp}}{C_T} \quad (17)$$

Even if the concentration of reactant A is high, the concentration factor, C_{fp}/C_T, controls the reaction rate in ice. In Figure 3, the concentration of reactant A in the micropockets is only twice the concentration in the solution. If the effect of the activation energy to depress the reaction rate is larger than the effect of freeze-concentration to increase the reaction rate, the reaction rate decreases.

Thus the reactions accelerated by freezing are as follows:

(i) second- or higher-order reactions,

(ii) low total initial concentration (e.g., low C_{T0}) and low reactant concentration (e.g., low [A]), and

(iii) small activation energy of the reaction.

This formulation clearly shows that reactions with a buffer solution or additives in order to adjust ion strength, zero- or first-order reactions, or reactions in the case of the high reactants

concentrations in order to accelerate the reactions cannot be accelerated in the ice.

The above mechanism can be applied to reactions accelerated due to the freeze-concentration effect. Several reactions are known to take place by the other mechanisms during freezing. For example, the pH is changed and hydrolysis reactions are accelerated.[4,24,33,34] In addition, solutes migrate from the ice to the solution even below the eutectic point, and reactions occur.[28,29] For solutes confined in the grain boundary, the circumstances are different from the solution (i.e., relatively low amounts of water molecules), and the reaction pathway is changed.[35] In order to clarify the chemistry in freezing completely, it is necessary to investigate these reaction mechanisms. Here, we explained the mechanism of the freeze-concentration effect and how it alters the kinetics of chemical reactions.

Application of the Present Kinetic Theory to the Reaction in the Unfrozen Solution in the Ice. The reaction of nitrite with dissolved oxygen is very fast in the frozen system. The reaction rate at −21 °C at pH 4.5 is about 200 000 times faster than that in the solution at 25 °C.[14] The reactions terminate when the entire sample is frozen and has established a thermal equilibrium at temperatures lower than −3 °C.[16] Therefore, the above theory was applied to the reaction after the entire sample was frozen at −0.5, −1, and −2 °C. Under these conditions, the reaction continues after the entire sample was frozen. The reaction of nitrous acid with dissolved oxygen is expressed as follows.

$$2HNO_2 + O_2 \rightarrow 2NO_3^- + 2H^+ \qquad (18)$$

In the calculation, we assume that the concentration of dissolved oxygen was constant and equilibrated with the partial pressure of the atmospheric oxygen. Air bubbles were formed in the micropocket,[36] and the composition of the bubbles were expected to be mainly N_2 and O_2. The dissolved oxygen that was consumed by the reaction would be supplied from the air bubbles in the unfrozen solution. Thus, the reaction can be treated as second-order kinetics, and the molar change, ΔC, can be considered as +2. Figure 6 shows the calculated results (black solid and broken lines) with the experimental results (black and white circles). In Figure 6, the time 0 represents the time when the entire sample was frozen. The initial concentration, temperature, and V_f were different in three cases. As shown in Figure 6, the results calculated by the proposed theory simulate the experimental results. The deviation of the calculated results for nitrite at −0.5 and −2 °C were observed. The reason is not clear, but some nitrites were already incorporated in ice crystals. In order to simulate the experimental results more precisely, the study of distribution coefficients of solutes into ice is required. Furthermore, in order to compare the present model with considering molar change by reaction to the model proposed by Pincock without considering molar change by reaction, the calculated results by the Pincok's model are also shown in Figure 6 (gray lines). The differences are very small, but the present model simulates the experimental results better than Pincock's model except for nitrite at −0.5 °C.

The reaction of thiosulfate with hydrogen peroxide is also accelerated by freezing.[20] The reaction mechanism in solution is reported as Scheme 1.[37,38] The calculation is very complicated. If we assume the effect of molar change can be ignored, the calculation becomes simple. The calculated results are shown in Figure 7 with the experimental results. The time 0 represents the time when the entire sample was frozen. The calculated results are in good agreement with the experimental results. In

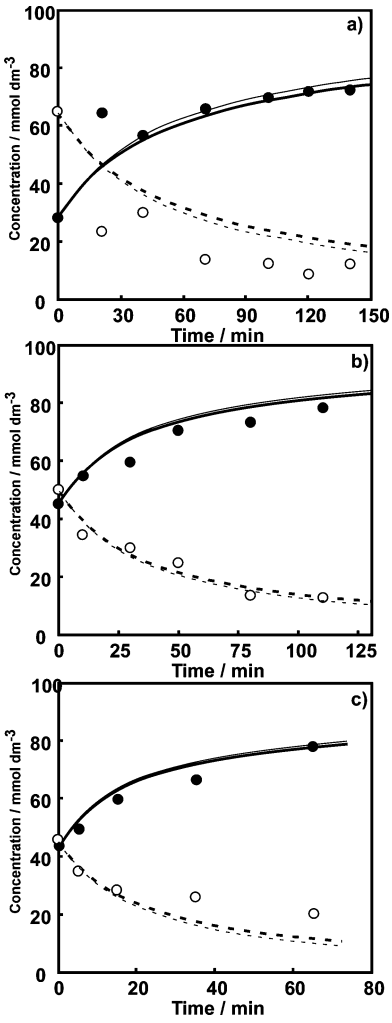

Figure 6. Time profile of the reaction of nitrous acid with dissolved oxygen in ice at (a) −0.5 °C, (b) −1.0 °C, and (c) −2.0 °C. The initial nitrous acid and dissolved oxygen concentrations are 1.00×10^{-4} and 4.5×10^{-4} mol dm^{-3}, respectively. The time zero in the figure is the time when the entire sample was frozen. The reaction proceeds during freezing. White circle: nitrite (nitrite ion + nitrous acid) in the experiment. Black circle: nitrate in the experiment. Broken lines: nitrite (nitrite ion + nitrous acid) in the calculation. Solid lines: nitrate in the calculation. Black lines: the present model. Gray lines: the model by Pincock.

SCHEME 1: Reaction Mechanism of the Reaction of Thiosulfate and Hydrogen Oxide

$$H_2O_2 + S_2O_3^{2-} \underset{k_{-1}}{\overset{k_1}{\rightleftharpoons}} HOS_2O_3^- + OH^-$$

$$H_2O_2 + HOS_2O_3^- \xrightarrow{k_2} 2HSO_3^- + H^+$$

$$S_2O_3^{2-} + S_2O_3 \xrightarrow{k_3} S_4O_6^{2-}$$

$$H_2O \underset{k_{-4}}{\overset{k_4}{\rightleftharpoons}} H^+ + OH^-$$

$$H_2O_2 + HSO_3^- \xrightarrow{k_5} SO_4^{2-} + H_2O + H^+$$

$$H_2O_2 + HSO_3^- + H^+ \xrightarrow{k_{5'}} SO_4^{2-} + H_2O + 2H^+$$

$$HSO_3^- \underset{k_{-6}}{\overset{k_6}{\rightleftharpoons}} H^+ + SO_3^{2-}$$

$$HOS_2O_3^- + H^+ \underset{k_{-7}}{\overset{k_7}{\rightleftharpoons}} S_2O_3 + H_2O$$

the experiments, $S_2O_3^{2-}$, SO_4^{2-}, sulfite, and $S_4O_6^{2-}$ were measured, but the intermediates, S_2O_3 and $HOS_2O_3^-$, were not measured. In the calculation, the sum of SO_4^{2-}, S_2O_3, and

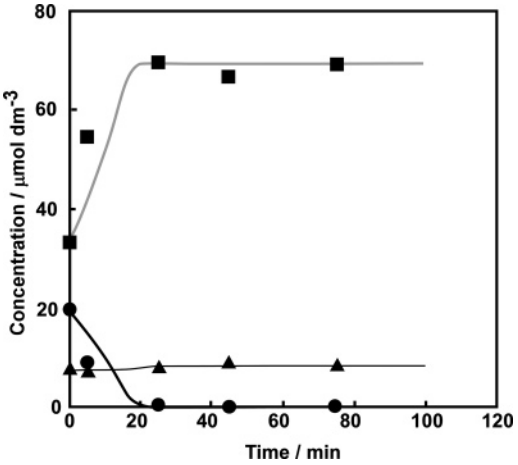

Figure 7. Time profile of the reaction of thiosulfate with hydrogen peroxide. The initial thiosulfate and hydrogen peroxide concentrations are 5.0×10^{-5} and 6.0×10^{-4} mol dm^{-3}, respectively. The time zero in the figure is the time when the entire sample was frozen. The reaction proceeds during freezing. Black circle: thiosuilfate in the experiment. Black square: $SO_4^{2-} + S_2O_3 + HOS_2O_3^-$ in the experiment. Black triangle: tetrathionate in the experiment. Black solid thick line: thiosuilfate in the calculation. Gray solid thick line: $SO_4^{2-} + S_2O_3 + HOS_2O_3^-$ in the calculation. Black fine line: tetrathionate in the calculation.

$HOS_2O_3^-$ concentrations is indicated as a gray line and shows good agreement with the measured sulfate change.

Conclusions

The present paper describes the modified acceleration model of reactions in ice. The model shows that the acceleration of reactions in ice is not unusual. The second- or higher-order reactions of low total concentration, and the reactions having a small activation energy are accelerated in ice.

The freezing process can be used for a new reaction method. After reactions, the products can be stored in ice if the temperature decreases below the eutectic points. Furthermore, photochemical reactions in ice in the polar regions are of interest recently.[27−31,39−43] The solutes are concentrated in the grain boundary of ice crystals and undergo various reactions. In the ice, the number of water molecules is much fewer than the solution, and reactions which are different from those in solution take place.[35] In order to understand the photochemistry of ice, it is necessary to elucidate the pH change during freezing and solvation of solutes in ice, in addition to the model we proposed here.

References and Notes

(1) Pincock, R. E. *Acc. Chem. Res.* **1969**, *2*, 97−103.
(2) Grant, N. H.; Clark, D. E.; Alburn, H. E. *J. Am. Chem. Soc.* **1961**, *83*, 4476−4477.
(3) Brown, W. D.; Dolov, A. *J. Food Sci.* **1963**, *28*, 211.
(4) Weatherburn, M. W.; Logan, J. E. *Clin. Chim. Acta* **1964**, *9*, 581−584.
(5) Alburn, H. E.; Grant, N. H. *J. Am. Chem. Soc.* **1965**, *87*, 4174−4177.
(6) Grant, N. H.; Alburn, H. E. *Science* **1965a**, *150*, 1589−1590.
(7) Grant, N. H.; Alburn, H. E. *Biochemistry* **1965b**, *4*, 1913−1916.
(8) Grant, N. H.; Alburn, H. E. *Nature* **1966**, *212*, 194.
(9) Lund, D. B.; Fennema, O.; Powrie, W. D. *J. Food Sci.* **1969**, *34*, 378−382.
(10) Fan, T.-Y.; Tannenbaum, S. R. *J. Agric. Food Chem.* **1973**, *21*, 967−969.
(11) Fennema, O. In *Water Relations of Foods*; Duckworth, R. B., Eds.; Academic Press: London, 1975; pp 539−556.
(12) Hatley, R. H. M.; Frank, F.; Day, H.; Byth, B. *Biophys. Chem.* **1986**a, *24*, 41−46.
(13) Hatley, R. H. M.; Frank, F.; Day, H. *Biophys. Chem.* **1986**b, *24*, 187−192.
(14) Takenaka, N.; Ueda, A.; Maeda, Y. *Nature* **1992**, *358*, 736−738.
(15) Takenaka, N.; Ueda, A.; Maeda, Y. *Proc. NIPR Symp. Polar Meterol. Glacial.* **1993**, *7*, 24−32.
(16) Takenaka, N.; Ueda, A.; Daimon, T.; Bandow, H.; Dohmaru, T.; Maeda, Y. *J. Phys. Chem.* **1996**, *100*, 13874−13884.
(17) Emoto, M.; Honda, K.; Yamazaki, N.; Mori, Y.; Fujieda, S. *Abstract(I) of the 79th Annual Meeting of the Japan Chemical Society 2001*; 2001, p 622, 3PA104 (in Japanese).
(18) Betterton, E. A.; Anderson, D. J. *J. Atmos. Chem.* **2001**, *40*, 171−189.
(19) Takenaka, N.; Furuya, S.; Sato, K.; Bandow, H.; Maeda, Y.; Furukawa, Y. *Int. J. Chem. Kinet.* **2003**, *35*, 198−205.
(20) Sato, K.; Furuya, S.; Takenaka, N.; Bandow, H.; Maeda, Y.; Furukawa, Y. *Bull. Chem. Soc. Jpn.* **2003**, *76*, 1139−1144.
(21) Arakaki, T.; Shibata, M.; Miyake, T.; Hirakawa, T.; Sakugawa, H. *Geochem. J.* **2004**, *38*, 383−388.
(22) Champion, D.; Simatos, D.; Kalogianni, E. P.; Cayot, P.; Le Meste, M. *J. Agric. Food Chem.* **2004**, *52*, 3399−3404.
(23) O'Driscoll, P.; Lang, K.; Minogue, N.; Sodeau, J. *J. Phys. Chem. A* **2006**, *110*, 4615−4618.
(24) Takenaka, N.; Tanaka, M.; Okitsu, K.; Bandow, H. *J. Phys. Chem. A* **2006**, *110*, 10628−10632.
(25) Cobb, A. W.; Gross G. W. *J. Electrochem. Soc.* **1969**, *116*, 796−804.
(26) Gross, G. W.; Wu, C.; Bryant, L.; McKee, C. *J. Chem. Phys.* **1975**, *62*, 3085−3092.
(27) Cho, H.; Shepson, P. B.; Barrie, L. A.; Cowin, J. P.; Zaveri, R. *J. Phys. Chem. B* **2002**, *106*, 11226−11232.
(28) Gudipati, M. S. *J. Phys. Chem. A* **2004**, *108*, 4412−4419.
(29) Ruzicka, R.; Baráková, L.; Klán, P. *J. Phys. Chem. B* **2005**, *109*, 9346−9353.
(30) Dubowski, Y.; Colussi, A. J.; Boxe, C.; Hoffmann, M. R. *J. Phys. Chem. A* **2001**, *106*, 6967−6971.
(31) Boxe, C.; Colussi, A. J.; Hoffmann, M. R.; Tan, D.; Mastromarino, J.; Case, A. T.; Sandholm, S. T.; Davis, D. D. *J. Phys. Chem. A* **2003**, *107*, 11409−11413.
(32) Kiovsky, T. E.; Pincock, R. E. *J. Am. Chem. Soc.* **1966**, *88*, 4704−4710.
(33) Bronsteyn, V. L.; Chernov, A. A. *J. Cryst. Growth* **1991**, *112*, 129−145.
(34) Heger, D.; Klánová, J.; Klán, P. *J. Phys. Chem. B* **2006**, *110*, 1277−1287.
(35) Klánová, J.; Klán, P.; Heger, D.; Holoubek, I. *Photochem. Photobiol. Sci.* **2003**, *2*, 1023−1031.
(36) Wang, Z.; Mukai, K.; Lee, I. J. *ISIJ Int.* **1999**, *39*, 553−562.
(37) Rábai, G.; Hamazaki, I. *Chem. Commun.* **1999**, 1965−1966.
(38) Kovács, K. M.; Rábai, G. *Phys. Chem. Chem. Phys.* **2002**, *4*, 5265−5269.
(39) Sumner, A. L.; Shepson, P. B. *Nature* **1999**, *398*, 230−233.
(40) Dubowski, Y.; Hoffmann, M. R. *Geophys. Res. Lett.* **2000**, *27*, 3321−3324.
(41) Hellebust, S.; Roddis, T.; Sodeau, J. R. *J. Phys. Chem. A* **2007**, *111*, 1167−1171.
(42) Boxe, C.; Colussi, A. J.; Hoffmann, M. R.; Murphy, J. G.; Wooldridge, P. J.; Bertram, T. H.; Cohen, R. C. *J. Phys. Chem. A* **2005**, *109*, 8520−8525.
(43) Boxe, C.; Colussi, A. J.; Hoffmann, M. R.; Perez, I. M.; Murphy, J. G.; Cohen, R. C. *J. Phys. Chem. A* **2006**, *110*, 3578−3583.